

Emergence of the molecular geometric phase from exact electron-nuclear dynamics

Rocco Martinazzo^{1,2,*}, Irene Burghardt³

¹*Department of Chemistry, Università degli Studi di Milano, Via Golgi 19, 20133 Milano, Italy**

²*Istituto di Scienze e Tecnologie Molecolari, CNR, via Golgi 19, 20133 Milano, Italy and*

³*Institute of Physical and Theoretical Chemistry, Goethe University Frankfurt, Max-von-Laue-Str. 7, D-60438 Frankfurt/Main, Germany*

Geometric phases play a crucial role in diverse fields. In chemistry they appear when a reaction path encircles an intersection between adiabatic potential energy surfaces and the molecular wavefunction experiences quantum-mechanical interference effects. This intriguing effect, closely resembling the magnetic Aharonov-Bohm effect, crucially relies on the adiabatic description of the dynamics, and it is uncertain whether and how it persists in an exact quantum dynamical framework. Recent works have shown that the geometric phase is an artifact of the adiabatic approximation, thereby challenging the perceived utility of the geometric phase concept in molecules. Here, we investigate this issue in an exact dynamical framework. We introduce instantaneous, *gauge* invariant phases separately for the electrons and for the nuclei, and use them to monitor the phase difference between the trailing edges of a wavepacket encircling a conical intersection. In this way we unambiguously assess the role of the geometric phase in the interference process and shed light on its persistence in molecular systems.

Introduction. Geometric phases represent fundamental concepts in the realms of physics and chemistry. They are closely associated with various phenomena, such as the quantum, the anomalous and the spin Hall effect [1, 2], the exotic physics of topological insulators [3, 4], dielectric polarization in crystals [2, 5–9], the Aharonov-Bohm effect [10], and conical intersections (CIs) in molecules [11–13]. Typically arising when the Hamiltonian of a system undergoes adiabatic changes with respect to a set of “environmental” parameters \mathbf{x} [14], geometric phases remain well defined even in scenarios involving non-adiabatic, non-cyclic and non-unitary evolutions [15–18]. In the case of molecules, geometric phases play a critical role around CIs between two or more potential energy surfaces. Their influence is subtle and eludes a description in the commonly adopted framework defined by the Born-Oppenheimer approximation. This is the case even if the molecular dynamics remains nearly adiabatic and does not occur in the proximity of the CI. Geometric phases affect the quantum interference of wavepackets encircling the CI [19, 20], no matter how close to the CI they move, and may have a significant impact on the reaction dynamics [21, 22], although cancellation effects may occur in the observables accessible in scattering experiments [23]. In these molecular problems, the Berry phase is often not just geometric but also topological, i.e., independent of both the dynamics and (to a large extent) of the path. In fact, it is the phase introduced in the pioneering works by Longuet-Higgins [24] and by Herzberg and Longuet-Higgins [25], and which is known to control the ordering of the energy levels in Jahn-Teller systems. However, these remarkable properties hinge crucially on the adiabatic approximation of the dynamics, raising the question whether and how they persist in an exact framework [26, 27].

Recent works [28, 29] addressed this question from a dynamical perspective, employing the same exact framework used in Refs. [26, 27], namely that provided by the exact factorization (EF) of the wavefunction [30, 31]. In our approach [29] we exploited a *gauge*-invariant formulation of the EF dynamics recently derived from quantum hydrodynamics (QHD) [32] to define geometric phases separately for both the nuclei and the electrons, for arbitrary paths γ in nuclear configuration space. These phases, henceforth $\Gamma_n[\gamma]$ and $\Gamma_{el}[\gamma]$, respectively for nuclei and electrons, always sum up to the phase difference of the *total* electron-nuclear ($e-n$) wavefunction at the end points of the path. When the path is closed the total phase difference vanishes [33] and the phases are just the opposite of each other, i.e., $-\Gamma_n^O[\gamma] = \Gamma_{el}^O[\gamma]$ where the superscript “O” indicates that the path is a loop. In this case, $\Gamma_{el}^O[\gamma]$ evolves in time according to a (reversed) Maxwell-Faraday induction law, with non-conservative forces arising from the electron dynamics that play the role of electromotive forces [29]. Furthermore, in the adiabatic limit, these forces are conservative, $\Gamma_{el}^O[\gamma]$ becomes stationary and the usual adiabatic geometric phase results. When the path is not closed, however, $\Gamma_n[\gamma]$ and $\Gamma_{el}[\gamma]$ are *distinct* contributions to the phase difference in the total $e-n$ wavefunction, which can be assigned, respectively, to a nuclear and an electronic *wavefunction*. The *gauge* choice which is *necessary* for this interpretation will emerge later on, when analyzing these phases in detail.

The purpose of this work is to provide a time-dependent perspective of the concept of geometric phase, i.e. to show how it emerges in the course of an exact dynamics and how it affects, under suitable conditions, the dynamics itself. To this end, we will focus on a model Jahn-Teller problem and exploit $\Gamma_n[\gamma]$ and $\Gamma_{el}[\gamma]$ introduced above to track the evolution of the phase differences that develop between the trailing edges of a wavepacket encircling the conical intersection. The path

* rocco.martinazzo@unimi.it

we choose is a “dynamical” path that moves in tandem with the nuclear probability density — in accordance to a quantum hydrodynamical description of the exact e - n dynamics [32] — in such a way that it is always “at rest” with the wavepacket itself and its endpoints indeed follow the trailing edges of the latter. We show that $\Gamma_n[\gamma]$ and $\Gamma_{\text{el}}[\gamma]$ entail key information about possible interference between different portions of the wavefunction. This is close in spirit to the analysis of geometric phase effects in adiabatic processes in which the slow variables are (or can be treated as) external parameters that are under full control of the experimenter. The key difference between the latter and the present problem is that in the first case the quantum vector describing the fast variables (the electrons) is the sole responsible for the phase changes, while in the second the slow variables (the nuclear degrees of freedom) participate in the dynamics and concur in defining the quantum state under scrutiny.

Non-adiabatic geometric phases. The exact factorization of the molecular wavefunction [30, 31] extends the fiber structure of the adiabatic approximation to arbitrary states, thereby enabling a natural extension of the adiabatic Berry phase. EF largely simplifies the description of the exact nuclear dynamics, in fact very close to an adiabatic theory (a $U(1)$ gauge theory) if not for the presence of a time-dependent connection. By contrast, the traditional Born-Huang expansion of the total wavefunction [34] gives rise to a much more complicated theory — for n coupled electronic states, a $U(n)$ gauge theory — albeit with a stationary (but non-Abelian) connection [35].

In the EF approach [30, 31] the wavefunction is represented exactly as

$$|\Psi\rangle = \int_{\mathbf{x}} d\mathbf{x} \psi(\mathbf{x}) |u(\mathbf{x})\rangle |\mathbf{x}\rangle \quad (1)$$

where $\{|\mathbf{x}\rangle\}$ is the position basis of the nuclear variables x^k ($k = 1, 2, \dots, N$), $|u(\mathbf{x})\rangle$ is the conditional electronic state at \mathbf{x} and $\psi(\mathbf{x})$ is the marginal probability amplitude for the nuclei, i.e. the “nuclear wavefunction”. For each configuration \mathbf{x} of the nuclei, the electronic state and the nuclear wavefunction can be obtained from the amplitude of the total e - n wavefunction at \mathbf{x} , upon noticing that the latter *is* an electronic state, though generally not normalized. Hence, upon imposing its normalization one defines the EF pair $\{|u(\mathbf{x})\rangle, \psi(\mathbf{x})\}$,

$$\langle \mathbf{x} | \Psi \rangle_{\mathbf{x}} = \psi(\mathbf{x}) |u(\mathbf{x})\rangle \equiv |\Psi(\mathbf{x})\rangle \langle u(\mathbf{x}) | u(\mathbf{x}) \rangle_{\text{el}} = 1 \quad (2)$$

up to a *gauge* choice, i.e. up to an arbitrary phase factor $e^{i\varphi}$ ($e^{-i\varphi}$) which can be used to redefine $|u(\mathbf{x})\rangle$ ($\psi(\mathbf{x})$) without affecting the total wavefunction [36]. This introduces a proper (i.e., single-valued) electronic “frame” for each nuclear configuration. We assume that this can be done smoothly in nuclear configuration space — hence, that the representation of the Berry connection in the chosen frame, $A_k = i \langle u | \partial_k u \rangle$ for $k = 1 - N$, is well defined — at least in the regions most relevant for the

dynamics [37]. At a wavefunction node $|\Psi(\mathbf{x})\rangle \equiv 0$, the electronic state is arbitrary and we assume that it is selected smoothly with its neighborhoods. Note that the total wavefunction can be considered *gauge* invariant, at least as long as the molecule is isolated and does not couple to external fields (e.g. an electromagnetic field).

The evolution of the EF pair of functions can be obtained from either the variational principle or projection operator techniques, as shown, respectively, in Refs. [30, 31] or Refs. [38, 39]. It is not needed here, though, since the key quantities of interest in this article require neither the evolution of the EF pair nor that EF is actually performed. The key information is that an exact factorization exists and that it introduces, at any time of interest, a proper electronic frame in nuclear configuration space. Indeed, this implies a phase quantization condition

$$\sum_k \oint_{\gamma} p_k dx^k = \sum_k \oint_{\gamma} (\pi_k + \hbar A_k) dx^k = 2\pi \hbar n \quad (3)$$

(with $n \in \mathbb{Z}$) which merely expresses the fact that the EF nuclear wavefunction ψ must be smooth around any loop γ in nuclear configuration space. Here, with $\hat{p}_k = -i\hbar\partial_k$ denoting the Schrödinger-representation canonical momentum, $p_k = \Re[(\hat{p}_k\psi)/\psi] \equiv \hbar\partial_k \arg \psi$ is the k^{th} derivative of the phase of the EF nuclear wavefunction and $\pi_k = p_k - \hbar A_k$ is the same component of the mechanical momentum $\boldsymbol{\pi}$ appearing in the quantum hydrodynamical description of the EF dynamics [32]. Furthermore, n is a topological value that describes the way the wavefunction phase possibly winds around a singularity: it is non-zero only if the singularity makes the domain multiply connected, otherwise γ can be shrunk to a single point and n must vanish. Importantly, the mechanical momentum and the quantization condition of Eq. 3 are *gauge*-invariant, even though p_k and A_k are not. In fact, $\boldsymbol{\pi}$ does not even require EF, it can be obtained from the total e - n wavefunction according to $\boldsymbol{\pi} \equiv \Re \langle \Psi(\mathbf{x}) | \hat{\mathbf{p}} | \Psi(\mathbf{x}) \rangle_{\text{el}} / n(\mathbf{x})$ — where $\hat{\mathbf{p}} = (\hat{p}_1, \hat{p}_2, \dots, \hat{p}_N)$ and $n(\mathbf{x}) = \langle \Psi(\mathbf{x}) | \Psi(\mathbf{x}) \rangle_{\text{el}}$ is the nuclear density.

The last observation, jointly with Eq. 3, allows one to introduce an instantaneous geometric phase for arbitrary paths, which reduces (modulo 2π) to the holonomy of the EF vector bundle when the path is closed (hence to the traditional Berry phase when the state is adiabatic). Specifically, as shown in Ref. [29], one can decompose the “total” phase difference $\Theta_{ba} = \arg \langle \Psi(\mathbf{x}_a) | \Psi(\mathbf{x}_b) \rangle$ between the endpoints \mathbf{x}_a and \mathbf{x}_b of a curve γ in nuclear configuration space as follows

$$\Theta_{ba} = \Gamma_n[\gamma] + \Gamma_{\text{el}}[\gamma] \quad (4)$$

where

$$\Gamma_{\text{el}}[\gamma] = \arg \langle u(\mathbf{x}_a) | u(\mathbf{x}_b) \rangle + \sum_k \int_{\gamma} A_k dx^k \quad (5)$$

is the Pancharatnam phase accumulated by the electronic vector from \mathbf{x}_a to \mathbf{x}_b along γ [15, 17, 18, 40, 41] and

$$\Gamma_n[\gamma] = \frac{1}{\hbar} \sum_k \int_\gamma \pi_k dx^k \quad (6)$$

is a nuclear phase. The decomposition is unique, since the above phases are *gauge* invariant, and it allows one to identify separate electronic and nuclear contributions to the phase difference of the total wavefunction. $\Gamma_{\text{el}}[\gamma]$ is indeed the phase acquired by the electronic state vector in the *parallel transport gauge* $|\tilde{u}\rangle$ defined by the condition $\sum_k \tilde{A}_k dx^k \equiv 0$, along the given curve [42]. Likewise, $\Gamma_n[\gamma]$ is the phase accumulated by the nuclear *wavefunction* $\tilde{\psi}$ in the same *gauge*, since $\sum_k \pi_k dx^k \equiv \sum_k \tilde{p}_k dx^k \equiv \hbar d(\arg \tilde{\psi})$, where tilde is used to denote quantities in the parallel transport *gauge*.

Hence, for a given curve γ , $\Gamma_{\text{el}}[\gamma]$ and $\Gamma_n[\gamma]$ single out, from the infinitely many *gauges* made possible by the EF, a specific *gauge* in which monitoring the “intrinsic” phase changes of the two subsystems. These correspond to *wavefunction* phases in this and only this gauge. This is also the *gauge* where geometric phase effects in the nuclear dynamics become manifest, since it is the most appropriate for neglecting the vector potential in the EF effective Hamiltonian \tilde{H}^{eff} for the nuclear wavefunction [30, 31, 38, 39], at least when the focus is on the dynamics along the given (open) path. When applying this approximation, i.e., when setting $A_k \equiv 0$ in \tilde{H}^{eff} , the resulting Hamiltonian becomes equivalent *in form* to the Born-Oppenheimer Hamiltonian, provided one further neglects the so-called diagonal corrections, i.e. disregard the effects of the *pseudo*-electric forces arising from the Fubini-Study metric. This represents the point of closest contact with BO dynamics. Notice however that the resulting effective Hamiltonian, freed of geometric effects, contains yet time-dependent electronic states in place of the stationary states that would appear in the BO limit.

For a loop, if a geometric phase is present, the electronic frame $|\tilde{u}\rangle$ is *improper*, meaning that is not single-valued anymore, and a smooth nuclear wavefunction satisfying the quantization condition of Eq. 3 does not exist. Rather, we have $-\Gamma_n^O[\gamma] = \Gamma_{\text{el}}^O[\gamma] = \arg \langle u_a | \tilde{u}_a \rangle$ and $\arg(\psi_a^* \tilde{\psi}_a) = -\hbar \Gamma_{\text{el}}^O[\gamma]$ becomes the boundary condition appropriate for the nuclear wavefunction in the parallel transport *gauge* [43]. This is also the case where departures from BO dynamics are larger, since the latter cannot account for the multi-valuedness of the wavefunction. Obviously, under such circumstances, a proper, smooth frame is more convenient for describing the nuclear dynamics. With this choice $\Gamma_{\text{el}}^O[\gamma]$ becomes an integral property of the electronic frame and the nuclear wavefunction satisfies the simpler condition of Eq. 3.

In practice, for a time-evolving wavepacket $|\Psi_t\rangle$ and a path γ_t — which possibly changes in time, too — the total phase Θ_{ab} is directly obtainable from the $e-n$ wavefunction amplitude at the endpoints of the path, while $\Gamma_n[\gamma_t]$ is readily available from the instantaneous momen-

tum field, $\boldsymbol{\pi}(\mathbf{x}, t) = \Re \langle \Psi_t(\mathbf{x}) | \hat{\mathbf{p}} | \Psi_t(\mathbf{x}) \rangle_{\text{el}} / n_t(\mathbf{x})$, upon integrating the latter along the path at the given t , see Eq. 6. Hence, the electronic phase can be obtained from the above two quantities, without requiring any explicit knowledge of a connection. The same momentum field $\boldsymbol{\pi}$ determines (through a mass tensor) the velocity field $\mathbf{v}(\mathbf{x}, t)$ of the nuclear probability fluid, hence the QHD trajectories $\dot{\mathbf{x}} = \mathbf{v}(\mathbf{x}, t)$ that dictate the evolution of any point \mathbf{x} of a “dynamical object” that moves in tandem with the fluid, for instance, our chosen paths. We stress that these are Bohmian nuclear trajectories [44] in the EF-based representation of the dynamics, i.e. they describe a Bohmian dynamics which accounts for the effects of both a quantum potential and the non-conservative forces arising from the electron dynamics. This settles the problem of obtaining geometric-phase related quantities from any available exact solution of the dynamics.

Model Jahn-Teller dynamics. We now focus on a 2-state model that highlights the key features of a molecular problem involving a CI. The nuclear system contains in general a number of degrees of freedom described by $\mathbf{x} \in \mathcal{M} \cong \mathbb{R}^N$ and the electronic Hamiltonian takes the general form $H_{\text{el}} = A(\mathbf{x})\sigma_0 + \mathbf{B}(\mathbf{x})\boldsymbol{\sigma}$, where $A(\mathbf{x})$ is a scalar, $\mathbf{B}(\mathbf{x}) \in \mathcal{N} \cong \mathbb{R}^3$ is an effective magnetic field, $\sigma_0 = \mathbb{I}_2$ is the 2x2 unit matrix and $\boldsymbol{\sigma} = (\sigma_x, \sigma_y, \sigma_z)$ is the vector of Pauli matrices. Here, we assume that a diabatic basis [45] $\{|1\rangle, |2\rangle\}$ has been introduced and represent the $e-n$ molecular wavefunction in spinor form. We set $B_z \equiv 0$ to mimic time-reversal invariance and make the adiabatic Berry curvature vanishing everywhere except at the CI seam (defined by the condition $\mathbf{B}(\mathbf{x}) = 0$). Under such circumstances, the adiabatic Berry phase becomes topological (in fact, it is the Longuet-Higgins phase [24, 25]), namely $(\pm)\pi$ for any path in \mathcal{N} space encircling the CI once, when the system is in the ground (excited) state. For concreteness, we consider 2+1 nuclear degrees of freedom ($\mathcal{M} \cong \mathbb{R}^3$) mimicking a one-dimensional CI seam, with parameter values appropriate for a molecular problem and a diagonal mass tensor, characterized by the nuclear mass $M = 1$ a.m.u.. Upon setting $A(\mathbf{x}) = \frac{1}{2}M\omega_x^2 x^2 + \frac{1}{2}M\omega_y^2 y^2$ and employing a linear vibronic coupling, $\mathbf{B} = \kappa_x x \mathbf{e}_1 + \kappa_y y \mathbf{e}_2$, the problem becomes effectively two-dimensional, in fact a standard, linear $E \otimes e$ Jahn-Teller model, with the CI seam represented by an isolated point, $\mathbf{x} = \mathbf{0}$. As for the parameters of the Hamiltonian, we set $\omega_x = \omega_y = \omega = 1000$ cm⁻¹ and $\kappa_x = \kappa_y = \kappa = 0.1$ a.u..

We solved the time-dependent Schrödinger equation for this problem using a standard Split-Operator algorithm in conjunction with Fast-Fourier-Transforms to go back and forth between real- and momentum-space. The wavefunction was represented on a fine grid (1024×1024), which was centered around the CI point and taken of length $20 a_0$ along each direction. A small time step of $\Delta t = 0.1$ a.u. was adopted to ensure a good sampling of the geometric phases over time. The initial wavefunction was obtained by combining a nuclear wavepacket $\psi_0(\mathbf{x})$ with a ground electronic state $|u_-(\mathbf{x})\rangle$, i.e. $\langle \mathbf{x} | \Psi_0 \rangle_{\mathcal{X}} =$

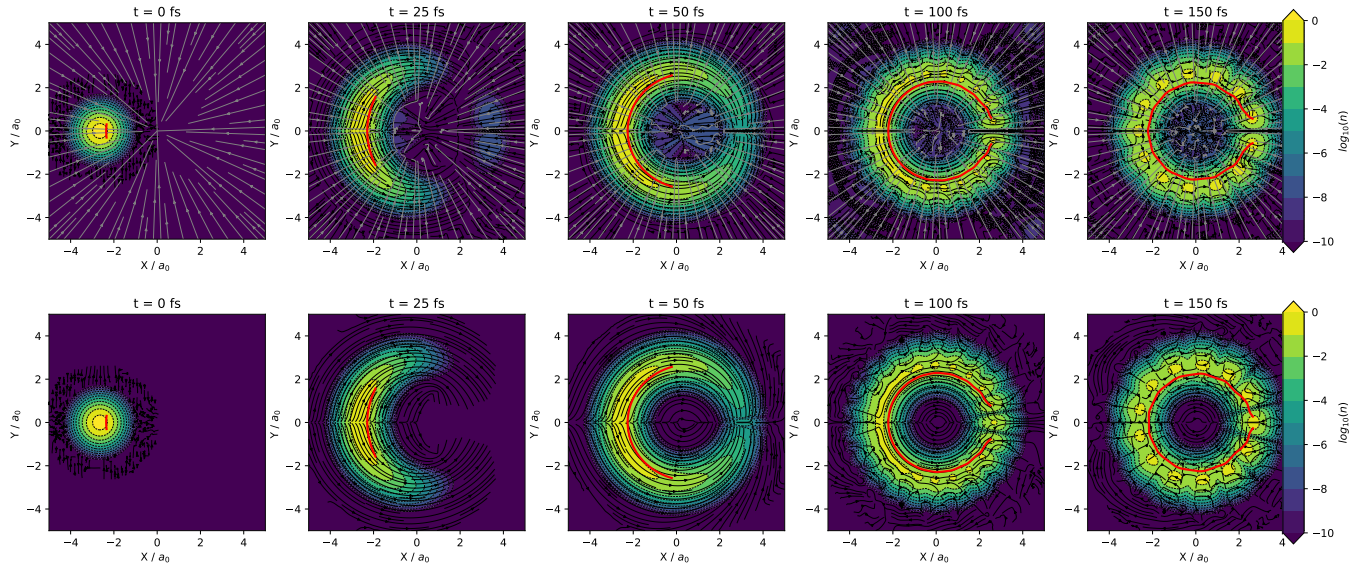


Figure 1. Evolution of an $e-n$ wavepacket encircling a conical intersection point between two adiabatic electronic states, located at the origin of the coordinate system. The top row shows the evolution of the nuclear density (color coded in a \log_{10} scale according to the colorbar on the right) as follows from a numerically exact solution of the time dependent Schrödinger equation for the 2-state model described in the main text (case (a)). The grey lines with arrows represent the field lines of the polarization field \mathbf{s} , which gives information about the local electronic states defined by the exact factorization of the wavefunction (see text for details). The bottom row shows similarly the evolution of the nuclear density in the Born-Oppenheimer approximation, when using the adiabatic ground-state energy and the same initial nuclear state of the exact dynamics. In each panel the red line represents the dynamical path used for computing the phases of Eqs. 4-6, while the black lines with arrows are the field lines of the nuclear momentum field $\boldsymbol{\pi}$.

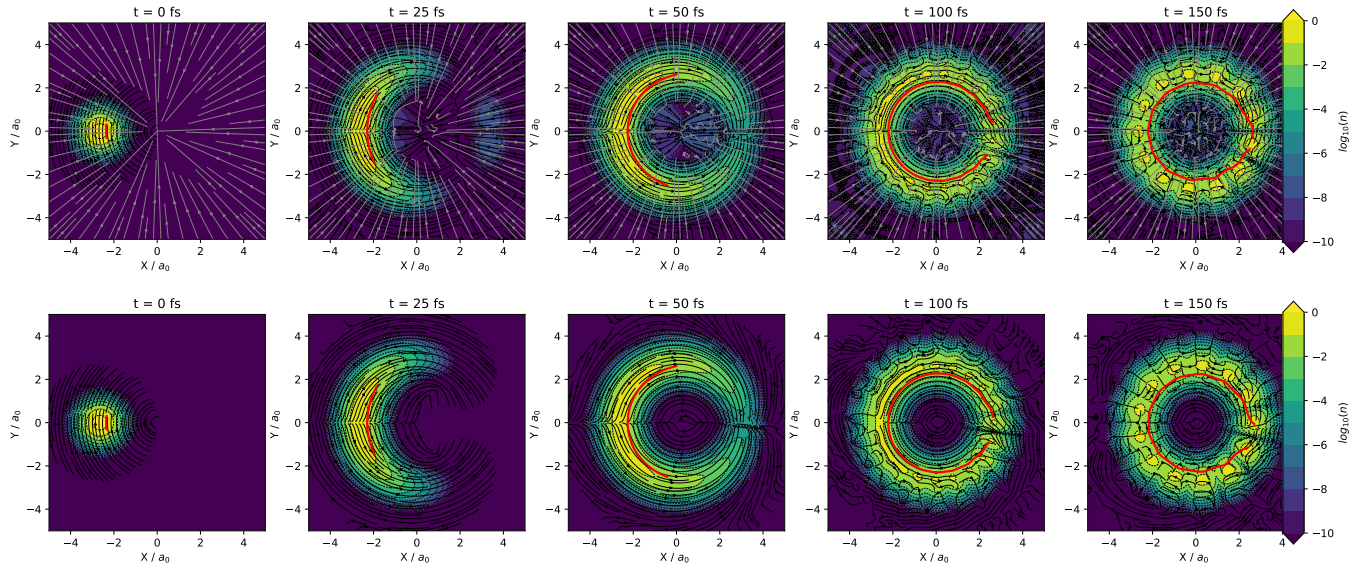


Figure 2. Same as in Fig. 1 for case (b), where the chosen initial state has a drift term in the clockwise direction (see main text for details).

$\psi_0(\mathbf{x})|u_-(\mathbf{x})\rangle$, where $\psi_0(\mathbf{x})$ was a Gaussian centered at $x_0 = -2\kappa/M\omega^2$ and $y_0 = 0$, with ground-state width along both x and y ($\Delta x = \Delta y = \sqrt{\hbar/2m\omega}$) and zero nominal momentum along both directions. Two slightly different initial states were considered, both using the

same $\psi_0(\mathbf{x})$ just described and differing only for the *gauge* choice of $|u_-(\mathbf{x})\rangle$ (see below). They both give rise to a dynamics which is very close to adiabatic, such that a comparison with Born-Oppenheimer dynamics is meaningful. Therefore, in parallel, we further performed calculations

in the BO approximation, employing the same set-up described above. To this end we set $\mathbf{B}(\mathbf{x}) = B(\mathbf{x})\sigma_z$ (where B is the magnitude of \mathbf{B}) and used a fictitious electronic state, namely $\chi(\mathbf{x}) \equiv [0, 1]$ in the chosen diabatic basis. As for the initial state wavefunction $\phi_0(\mathbf{x})$ appropriate for this problem we made sure that it represented the *same* (nuclear) state used in the exact problem, as described in the following.

A first initial state, henceforth case (a), was obtained with the *gauge* choice $|u_-(\mathbf{x})\rangle = (e^{-i\phi/2}|1\rangle - e^{i\phi/2}|2\rangle)/\sqrt{2}$ where ϕ is the azimuthal angle of the position vector \mathbf{x} . Even though this is an improper electronic frame presenting a discontinuity on the positive x axis this is irrelevant for our purposes, since $\psi_0(\mathbf{x})$ localizes on the negative x axis. In fact, this is a parallel transport frame for any open path not crossing the positive x axis, since the corresponding Berry vector potential vanishes everywhere in \mathbb{R}^2 except on that semi-axis, where it is singular (in \mathbb{R}^3 this would be the direction of the so-called Dirac line). The corresponding BO counterpart of this initial state was then set to $\phi_0(\mathbf{x}) \equiv \psi_0(\mathbf{x})$. This choice ensures that the two dynamics share the same density $n(\mathbf{x})$ and the same momentum field $\boldsymbol{\pi}(\mathbf{x})$ at the initial time [46]. Notice that $\boldsymbol{\pi}(\mathbf{x}) \equiv \mathbf{0}$ at $t = 0$ (where $\boldsymbol{\pi}$ is well-defined), since $\psi_0(\mathbf{x})$ is real and there is no contribution to the mechanical momentum coming from the Berry connection. This defines a state that remains symmetric (even) with respect to mirror reflections about the x axis (see Fig. 1).

In a second initial state, henceforth case (b), the *gauge* was fixed with the proper choice $|u_-(\mathbf{x})\rangle = (-|1\rangle + e^{i\phi}|2\rangle)/\sqrt{2}$, which is a special case of a standard parametrization of the Bloch sphere, often used to describe the ground state of a spin in a magnetic field. This parametrization reads as $|u_-\rangle = \sin(\theta/2)|1\rangle - e^{i\phi}\cos(\theta/2)|2\rangle$, for the field along the unit vector $\mathbf{b} = \cos\phi\sin\theta\mathbf{e}_1 + \sin\phi\sin\theta\mathbf{e}_2 + \cos\theta\mathbf{e}_3$, where θ and ϕ are the usual latitude and longitude angles of the spherical coordinates in \mathbb{R}^3 [47]. It is regular everywhere on the Bloch sphere except for $\theta = 0$, hence the Dirac line of the corresponding Berry vector potential lies along the positive z axis and it is harmless for our problem (where $\theta \equiv \pi/2$). This comes at a price of introducing a non-vanishing vector-potential contribution to the initial momentum $\boldsymbol{\pi}$, a clockwise vortex structure centered at the CI point, that causes a drift of the system in the same sense [48] (Fig. 2). In this case, $|\tilde{u}_-\rangle = e^{-i\phi/2}|u_-\rangle$ would be needed to define the parallel transport *gauge*, hence $\phi_0(\mathbf{x}) = \tilde{\psi}_0(\mathbf{x}) = e^{i\phi/2}\psi_0(\mathbf{x})$ is our corresponding choice of the initial state for the BO dynamics. Again, this ensures that not only the same nuclear density $n(\mathbf{x}) = |\psi_0(\mathbf{x})|^2$ but also the same momentum field $\boldsymbol{\pi}(\mathbf{x})$ are defined at initial time for the two dynamics.

The resulting dynamics is very similar in the two cases: the wavepacket, initially located on one side of the CI point, spreads along the valley of the ‘‘Mexican hat’’ potential and its trailing edges meet each other and start interfering at time $t \approx 50 fs$, after which the wavepacket

covers more or less uniformly the valley, with a time-varying interference pattern (Figs. 1 and 2). The dynamics is adiabatic to a large extent, as a visual inspection of the field lines of the polarization field $\mathbf{s}(\mathbf{x})$ suggests and a more detailed analysis of the populations confirms (not reported). The vector field $\mathbf{s}(\mathbf{x})$ characterizes, in a *gauge* invariant way, the local electronic states defined by the EF of the total wavefunction, namely *via* $\rho_{\text{el}}(\mathbf{x}) = (\mathbb{I}_2 + \mathbf{s}(\mathbf{x})\boldsymbol{\sigma})/2$, where $\rho_{\text{el}}(\mathbf{x})$ is the matrix representation (in the chosen diabatic basis) of the conditional density operator $\hat{\rho}_{\text{el}}(\mathbf{x}) = |u(\mathbf{x})\rangle\langle u(\mathbf{x})|$, \mathbb{I}_2 is the unit 2×2 matrix and $\boldsymbol{\sigma}$ is the vector of Pauli matrices (for an adiabatic ground / excited state the polarization field reads, in our set-up, as $\mathbf{s}_{\mp}(\mathbf{x}) = \mp \mathbf{x}/\|\mathbf{x}\|$). The interference patterns in Figs. 1 and 2 depend on the details of the initial state, as the evolution of a dynamical path tied to the nuclear probability density makes evident (red line). Importantly, the pattern is reversed compared to the BO dynamics, a clear signature of geometric (topological) phase effects. The subtle differences between case (a) and case (b) (at the same level of description) can be revealed (by inspection) only in the path dynamics, and follow from the behavior of the phases introduced in the previous Section, as we now show.

Fig. 3 shows the nuclear ($\Gamma_{\text{n}}[\gamma]$), electronic ($\Gamma_{\text{el}}[\gamma]$) and total (Θ_{ab}) phase difference between the end points of the probe path that moves in tandem with the nuclear probability fluid and that was started as an arc centered at the initial wavepacket position (leftmost panels in Figs. 1 and 2). The behavior of the electronic phase – only relevant for the exact dynamics – is essentially the same, irrespective of the initial state, for our quasi-adiabatic dynamics around the CI point. The phase remains constant up to about $50 fs$, when the path becomes approximately a semicircle and the phase changes abruptly to $\pi \pmod{2\pi}$. This is also the limiting value that the phase takes when artificially closing the path after the transition point (i.e., when closing the path encompasses the CI point), and $\Gamma_{\text{el}}[\gamma]$ is seen to keep this value for $t \geq 50 fs$. This distinctive behavior of $\Gamma_{\text{el}}[\gamma]$ is a feature of the Pancharatnam phase of Eq. 5 that is easily seen to be operative already on the Bloch sphere, when parallel transporting vectors along great circles. For instance, when parallel transporting a ground-state vector $|u_a\rangle$ along the ϕ_0 meridian line $[0, 1] \ni s \rightarrow (s\pi, \phi \equiv \phi_0)$, up to the south pole, and back to the north pole along the antimeridian line $[0, 1] \ni s \rightarrow (\pi(1-s), \phi \equiv \phi_0 + \pi)$ to give $|\tilde{u}_a\rangle = -|u_a\rangle$. Indeed, using the above mentioned parameterization of the Bloch sphere – i.e., $|u_-\rangle = \sin(\theta/2)|1\rangle - e^{i\phi}\cos(\theta/2)|2\rangle$ – the line integral does not contribute to the phase since \mathbf{A} lies on latitude lines while, on the other hand, $\arg\langle u_-(0, \phi_0)|u_-(\theta, \phi)\rangle$ undergoes a sudden π jump when traversing the south pole. Changing the *gauge* makes the calculation a bit longer but does not affect the final result, since $\Gamma_{\text{el}}[\gamma]$ is *gauge* invariant.

Now, in the previous example the south pole is the point where the transported vector $|\tilde{u}_b\rangle$ is orthogonal

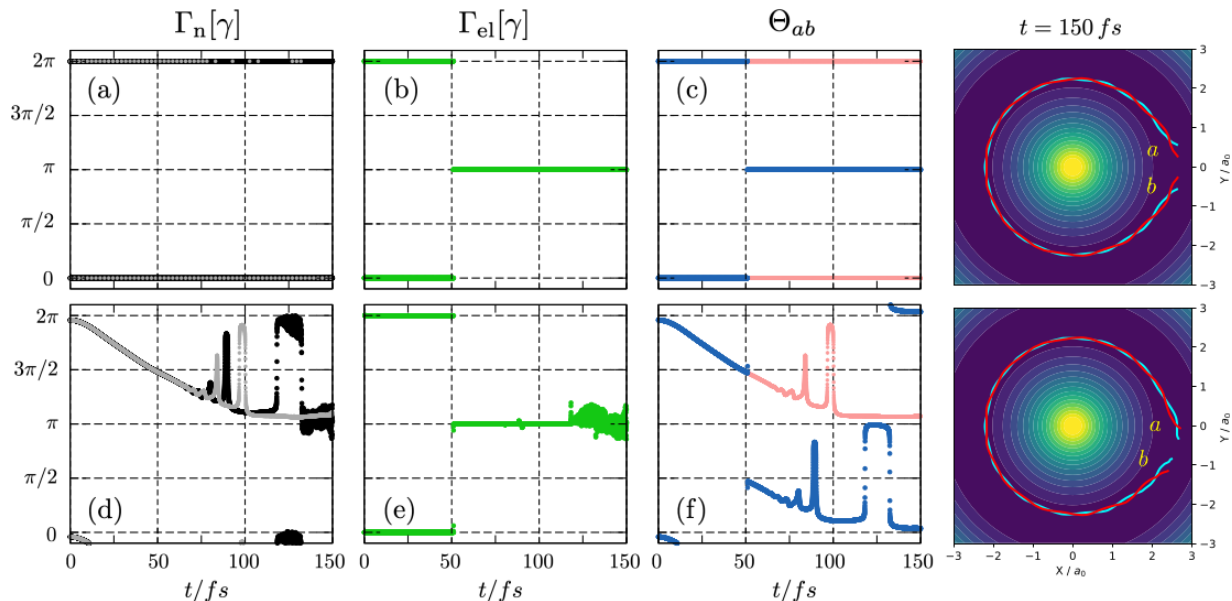


Figure 3. Phase differences between the endpoints a and b of the dynamical paths shown in Figs. 1-2. Panels (a-c) for Fig. 1 and panels (d-f) for Fig. 2. Panels (a) and (d) display the nuclear phase $\Gamma_n[\gamma]$ (black), (b,e) the electronic phase $\Gamma_{el}[\gamma]$ (green symbols) and (c,f) the total phase difference Θ_{ab} (light blue). Also shown are the results obtained from the Born-Oppenheimer dynamics, grey symbols in (a,d) and red symbols in (c,f). Data are shown with their $\pm 2\pi$ images for displaying purposes. The two rightmost panels show the paths at $t = 150 fs$, for the exact (cyan) and for the Born-Oppenheimer (red) dynamics, superimposed to a color map of the adiabatic, ground-state potential energy surface and with a, b labeling the endpoints of the curves.

to $|u_a\rangle$ and the phase $\arg\langle u_a|\tilde{u}_b\rangle$ is ill defined. This is the way the non-trivial Berry phase is generated when traveling along the great circle. In other words, the -1 (topological) phase factor does not build up continuously along the path, rather it is suddenly acquired when the state vector becomes orthogonal to the initial one. This is precisely what happens with the EF local electronic states attached to the endpoints of our dynamical path, when the latter is stretched for approximately half of a circle length along the valley of the ground-state potential, since the dynamics is essentially adiabatic and $\Gamma_{el}[\gamma]$ tracks the phase changes in the parallel transport *gauge*.

The behavior of the nuclear phase $\Gamma_n[\gamma]$, on the other hand, does depend on the initial state, being intimately related to the ensuing nuclear dynamics which is slightly different in the two cases, because of the absence (case (a)) or presence (case (b)) of a non-vanishing momentum field $\boldsymbol{\pi}$ at initial time. In case (a) the line integral of Eq. 6 vanishes by symmetry, whereas in case (b) the endpoints of the path travel at different velocities and cancellation of terms cannot occur. The behaviour is however essentially the same as in the Born-Oppenheimer dynamics, at least as long as the path endpoints—which, we recall, are closely related to the trailing edges of the wavepacket—are sufficiently far apart. This is due to the fact, mentioned above, that the phase takes the meaning of nuclear wavefunction phase in the parallel transport *gauge*, where the effective Hamiltonian \hat{H}^{eff} describing the evolution of the marginal probability amplitude in the EF

approach looks very similar to a BO Hamiltonian. This implies that the two dynamics are (locally) very similar to each other. Notice that for the problem discussed here the parallel transport condition (in the adiabatic limit) is topological, too, meaning that $\mathbf{A} = \mathbf{0}$ is a condition that defines a “global” parallel transport *gauge*, that does not depend on the chosen path [49].

In fact, the exact dynamics starts departing from the BO dynamics only when the trailing edges of the wavepacket come close to each other and interfere, as dictated by the *total* phase difference Θ_{ab} (Fig. 3 (c,f)). For the BO dynamics $\Theta_{ab} \equiv \Gamma_n[\gamma]$ (in Fig. 3 to within the numerical accuracy of the computation of the line integral of Eq. 6) while for the exact dynamics $\Theta_{ab} \approx \Gamma_n[\gamma] + \pi$. Hence, in case (a) (see Fig. 3 (c)) the wavepacket develops a node in the exact dynamics which is absent in the BO dynamics. This is manifest in the different behavior of the path endpoints, which is summarized in the top right panel of Fig. 3. On the other hand, in case (b) (see Fig. 3 (f)) it is the BO dynamics that presents a node, since in the exact dynamics the edges of the wavepacket can be smoothly merged due to $\Theta_{ab} \approx 0 \pmod{2\pi}$. This is clearly seen in the maps shown in the rightmost panels of Figs. 1 and 2, that display the nuclear density (in a \log_{10} scale) at long time.

We stress that the phases of Fig. 3 are *open-path* phases, for which the parallel transport *gauge* remains smooth all over the path and $\Gamma_n[\gamma]$, $\Gamma_{el}[\gamma]$ can be associated to single-valued nuclear and electronic wavefunc-

tions. Whether we artificially close the paths by bringing the endpoints a and b closer together, the *limiting* total phase difference Θ_{ab} depends on the possible presence of a nodal line crossing the path, $\Theta_{ab} \rightarrow 0$ without nodes and $\Theta_{ab} \rightarrow \pi$ for a node [50]. This “ π contribution” appearing in Θ_{ab} when a node is present parallels the δ -like term that arises in the momentum field π along a *closed*-path that crosses a nodal line. For instance, if $\psi(x, y) = 0$ in some interval of the positive x axis, then $\psi(x, y) \approx a(x)y$ holds around that axis (for $a(x) = (\partial_y \psi)(x, 0)$) and $\pi_y = \hbar \Im(1/y) = \pm \hbar \pi \delta(y)$, when the singularity is circumvented by deforming the path in the complex y plane. This means that, when a node develops between the endpoints of the curve, a π contribution would emerge from the very act of closing the path, i.e., when replacing $\Gamma_n[\gamma]$ with $\Gamma_n^O[\gamma]$. This would occur for the exact dynamics in panel (a) of Fig. 3 and for the BO dynamics in panel (d) of the same figure, and would formally enforce the condition $\Theta_{ab} = 0$, irrespective of the presence or absence of a nodal line. The implicit assumption is that the EF electronic state at the node (that, we recall, is arbitrary) is chosen smoothly, such that $\lim_{b \rightarrow a} \Gamma_{el}[\gamma] = \Gamma_{el}^O[\gamma]$.

Overall, the above results confirm elementary arguments about the topological contributions of the electrons to the total phase difference between the trailing

edges of a wavepacket encircling the CI. The choice of the initial state, though, is seen to play a distinctive role in determining whether a perfect destructive interference can or cannot occur between the edges. Noteworthy is that in case (b), an “attempt” to form a node is evident at $t \approx 125 fs$ (Fig. 3, panels (d) and (f)), but this fails since the broken symmetry of the initial state prevents perfect cancellation of contributions.

Finally, we remark that it is the existence of situations like cases (b) that makes inclusion of geometric phases not straightforward in typical mixed quantum-classical methods [51, 52] where electrons are treated quantumly and nuclei classically.

Conclusions. We have investigated molecular geometric phase effects from an *exact* quantum dynamical perspective, by defining *gauge* invariant nuclear and electronic phase differences, which are valid for arbitrary electronic states and for arbitrary paths in nuclear configuration space. We have shown that these phases may reveal key information about the wavefunction dynamics and the effects of a geometric phase, thereby providing a firm basis for the existence of geometric phase effects in molecules beyond the adiabatic approximation, and support for the elementary arguments often invoked in their explanation.

-
- [1] S. M. Girvin and K. Yang, Modern Condensed Matter Physics, Modern Condensed Matter Physics [10.1017/9781316480649](https://doi.org/10.1017/9781316480649) (2019).
- [2] D. Vanderbilt, Berry Phases in Electronic Structure Theory: Electric Polarization, Orbital Magnetization and Topological Insulators, Berry Phases in Electronic Structure Theory [10.1017/9781316662205](https://doi.org/10.1017/9781316662205) (2018).
- [3] M. Z. Hasan and C. L. Kane, Colloquium: Topological insulators, *Reviews of Modern Physics* **82**, 3045 (2010).
- [4] C. L. Kane, Topological Band Theory and the Z2 Invariant, *Contemporary Concepts of Condensed Matter Science* **6**, 3 (2013).
- [5] R. Resta, Theory of the electric polarization in crystals, *Ferroelectrics* **136**, 51 (1992).
- [6] R. D. King-Smith and D. Vanderbilt, Theory of polarization of crystalline solids, *Physical Review B* **47**, 1651 (1993).
- [7] R. Resta, Macroscopic polarization in crystalline dielectrics: the geometric phase approach, *Reviews of Modern Physics* **66**, 899 (1994).
- [8] R. Resta, Manifestations of Berry’s phase in molecules and condensed matter, *Journal of Physics: Condensed Matter* **12**, R107 (2000).
- [9] D. Xiao, M. C. Chang, and Q. Niu, Berry phase effects on electronic properties, *Reviews of Modern Physics* **82**, 1959 (2010), [arXiv:0907.2021](https://arxiv.org/abs/0907.2021).
- [10] Y. Aharonov and D. Bohm, Significance of electromagnetic potentials in the quantum theory, *Physical Review* **115**, 485 (1959).
- [11] C. A. Mead, The geometric phase in molecular systems, *Reviews of Modern Physics* **64**, 51 (1992).
- [12] D. R. Yarkony, Diabolical conical intersections, *Reviews of Modern Physics* **68**, 985 (1996).
- [13] B. K. Kendrick, Geometric phase effects in chemical reaction dynamics and molecular spectra, *Journal of Physical Chemistry A* **107**, 6739 (2003).
- [14] M. Berry, Quantal phase factors accompanying adiabatic changes, *Proceedings of the Royal Society of London. A. Mathematical and Physical Sciences* **392**, 45 (1984).
- [15] B. Simon, Holonomy, the Quantum Adiabatic Theorem, and Berry’s Phase, *Physical Review Letters* **51**, 2167 (1983).
- [16] Y. Aharonov and J. Anandan, Phase change during a cyclic quantum evolution, *Physical Review Letters* **58**, 1593 (1987).
- [17] R. Simon and N. Mukunda, Bargmann invariant and the geometry of the G uy effect, *Physical Review Letters* **70**, 880 (1993).
- [18] N. Mukunda and R. Simon, Quantum Kinematic Approach to the Geometric Phase. I. General Formalism, *Annals of Physics* **228**, 205 (1993).
- [19] S. C. Althorpe, General explanation of geometric phase effects in reactive systems: Unwinding the nuclear wave function using simple topology, *Journal of Chemical Physics* **124**, [10.1063/1.2161220](https://doi.org/10.1063/1.2161220) (2006).
- [20] C. H. Valahu, V. C. Olaya-Agudelo, R. J. MacDonell, T. Navickas, A. D. Rao, M. J. Millican, J. B. P erez-S anchez, J. Yuen-Zhou, M. J. Biercuk, C. Hempel, T. R. Tan, and I. Kassal, Direct observation of geometric-phase interference in dynamics around a conical intersection, *Nature Chemistry* **2023**, 1 (2023).
- [21] D. Yuan, Y. Huang, W. Chen, H. Zhao, S. Yu, C. Luo,

- Y. Tan, S. Wang, X. Wang, Z. Sun, and X. Yang, Observation of the geometric phase effect in the $\text{H}+\text{HD} \rightarrow \text{H}_2+\text{D}$ reaction below the conical intersection, *Nature Communications* **2020** 11:1 **11**, 1 (2020).
- [22] B. K. Kendrick, J. Hazra, and N. Balakrishnan, The geometric phase controls ultracold chemistry, *Nature Communications* **2015** 6:1 **6**, 1 (2015).
- [23] J. C. Juanes-Marcos, S. C. Althorpe, and E. Wrede, Chemistry: Theoretical study of geometric phase effects in the hydrogen-exchange reaction, *Science* **309**, 1227 (2005).
- [24] H. C. Longuet-Higgins, U. Öpik, M. H. L. Pryce, and R. A. Sack, Studies of the Jahn-Teller effect .II. The dynamical problem, *Proceedings of the Royal Society of London. Series A. Mathematical and Physical Sciences* **244**, 1 (1958).
- [25] G. Herzberg and H. C. Longuet-Higgins, Intersection of potential energy surfaces in polyatomic molecules, *Discussions of the Faraday Society* **35**, 77 (1963).
- [26] S. K. Min, A. Abedi, K. S. Kim, and E. K. Gross, Is the molecular berry phase an artifact of the Born-Oppenheimer approximation?, *Physical Review Letters* **113**, 263004 (2014), [arXiv:1402.0227](#).
- [27] R. Requist, F. Tandetzky, and E. K. Gross, Molecular geometric phase from the exact electron-nuclear factorization, *Physical Review A* **93**, 042108 (2016).
- [28] L. M. Ibele, E. Sangiogo Gil, B. F. E. Curchod, and F. Agostini, On the Nature of Geometric and Topological Phases in the Presence of Conical Intersections, *The Journal of Physical Chemistry Letters* **14**, 11625 (2023).
- [29] R. Martinazzo and I. Burghardt, Dynamics of the molecular geometric phase, (2023), [arXiv:2312.02823](#).
- [30] A. Abedi, N. T. Maitra, and E. K. U. Gross, Exact Factorization of the Time-Dependent Electron-Nuclear Wave Function, *Physical Review Letters* **105**, 123002 (2010).
- [31] A. Abedi, N. T. Maitra, and E. K. U. Gross, Correlated electron-nuclear dynamics: Exact factorization of the molecular wavefunction, *The Journal of Chemical Physics* **137**, 22A530 (2012).
- [32] R. Martinazzo and I. Burghardt, Quantum hydrodynamics of coupled electron-nuclear systems, [arXiv preprint](#) , **2310.08766** (2023), [arXiv:2310.08766](#).
- [33] Strictly speaking this holds unless there is a node at the base point of the path where the phase difference is considered. We shall address this issue in more detail below.
- [34] A. Bohm, *Quantum Mechanics: Foundations and Applications*, Theoretical and Mathematical Physics (Springer, 2001) p. 688.
- [35] C. Wittig, Geometric phase and gauge connection in polyatomic molecules, *Physical Chemistry Chemical Physics* **14**, 6409 (2012).
- [36] In Eq. 2 the subscript X (el) indicates that integration is performed over nuclear (electronic) variables only.
- [37] In other words, we assume that we can select a normalized section of the bundle that is smooth almost everywhere. Notice that there is always the possibility of having “essential” discontinuities that cannot be cured by any *gauge* choice. This happens, for instance, when $|\Psi\rangle$ represents an adiabatic state with a CI, since in that case the electronic state is ill-defined right at the CI seam. We assume $\langle \Psi(\mathbf{x}) | \Psi(\mathbf{x}) \rangle = 0$ there, otherwise the nuclear derivatives $\partial_j |\Psi(\mathbf{x})\rangle$'s would be singular.
- [38] R. Martinazzo and I. Burghardt, Quantum Dynamics with Electronic Friction, *Physical Review Letters* **128**, 206002 (2022), [arXiv:2108.02622](#).
- [39] R. Martinazzo and I. Burghardt, Quantum theory of electronic friction, *Physical Review A* **105**, 052215 (2022).
- [40] A. K. Pati, New derivation of the geometric phase, *Physics Letters A* **202**, 40 (1995).
- [41] A. K. Pati, Adiabatic Berry Phase and Hannay Angle for Open Paths, *Annals of Physics* **270**, 178 (1998), [arXiv:9804057 \[quant-ph\]](#).
- [42] It is always possible to find such a *gauge* for a given curve, since $|\tilde{u}\rangle = e^{i\varphi} |u\rangle$ implies $i \sum_k \langle \tilde{u} | \partial_k \tilde{u} \rangle dx^k = -d\varphi + i \sum_k \langle u | \partial_k u \rangle dx^k$, i.e. $\varphi = i \sum_k \int_\gamma A_k dx^k$.
- [43] To avoid confusion, the *gauge* transformation needed to turn a regular frame into a parallel transport *gauge* is singular, since it is not single-valued everywhere. Hence, the momentum field and the quantization condition of Eq. 3 do change under this kind of transformations.
- [44] P. R. Holland, The Quantum Theory of Motion: An Account of the de Broglie-Bohm Causal Interpretation of Quantum Mechanics, *The Quantum Theory of Motion* **10.1017/CBO9780511622687** (1993).
- [45] H. Köppel, W. Domcke, and L. S. Cederbaum, Multimode Molecular Dynamics Beyond the Born-Oppenheimer Approximation (John Wiley & Sons, Ltd, 1984) pp. 59–246.
- [46] Strictly speaking this is true *almost* everywhere and, in particular, in the regions of nuclear configuration space where it is most relevant, i.e. where $n(\mathbf{x})$ is sizable.
- [47] The more common parametrization is for the + (i.e. excited) state, where the spin is directed along the field axis. It is related to the one given here by a reversal of \mathbf{b} , i.e. $\theta \rightarrow \pi - \theta$ and $\phi \rightarrow \phi + \pi$.
- [48] A simple calculation shows that $\boldsymbol{\pi} = -\hbar/2r \mathbf{e}_\phi$, where $r = |\mathbf{x}|$ and \mathbf{e}_ϕ is the unit vector along the ϕ coordinate.
- [49] The condition $\nabla \times \mathbf{A} = \mathbf{0}$ allows one to write $\mathbf{A} = \nabla\varphi$ in any simply connected subdomain, where φ is a scalar. Hence, for any path *not* encircling the CI, $|u\rangle \rightarrow e^{i\varphi} |u\rangle$ defines the parallel transport *gauge*, $\mathbf{A} \rightarrow -\nabla\varphi + \mathbf{A} = \mathbf{0}$.
- [50] Notice that a node $|\Psi(\mathbf{x})\rangle = 0$ makes the phase $\Theta_{ab} = \arg \langle \Psi(\mathbf{x}_a) | \Psi(\mathbf{x}) \rangle$ no longer continuous.
- [51] T. R. Nelson, A. J. White, J. A. Bjorgaard, A. E. Sifain, Y. Zhang, B. Nebgen, S. Fernandez-Alberti, D. Mozyrsky, A. E. Roitberg, and S. Tretiak, Non-adiabatic Excited-State Molecular Dynamics: Theory and Applications for Modeling Photophysics in Extended Molecular Materials, *Chemical Reviews* **120**, 2215 (2020).
- [52] Y. Shu and D. G. Truhlar, Decoherence and Its Role in Electronically Nonadiabatic Dynamics, *Journal of Chemical Theory and Computation* **19**, 395 (2023).